Version of record: https://doi.org/10.1016/j.ifacol.2021.06.111
Available online at www.sciencedirect.com
ScienceDirect
IFAC Papers Online CONFERENCE PAPER ARCHIVE
IFAC PapersOnLine 54-9 (2021) 521–526

Modeling protein concentrations in cycling cells using stochastic hybrid systems ⋆

Zahra Vahdat[1] **Zikai Xu**[1] **Abhyudai Singh**[1,2]

[1] *Department of Electrical and Computer Engineering, University of Delaware, Newark, DE 19716 USA*
e-mail: zahravd@udel.edu, zikai@udel.edu
[2] *Department of Biomedical Engineering, Department of Mathematical sciences, Center for Bioinformatics and Computational Biology, University of Delaware, Newark, DE 19716 USA*
e-mail: absingh@udel.edu

Abstract: We analyze a class of time-triggered stochastic hybrid systems where the state-space evolves as per a linear time-invariant dynamical system. This continuous-time evolution is interspersed with two kinds of stochastic resets. The first reset occurs based on an internal timer that measures the time elapsed since it last occurred. Whenever the first reset occurs, the states-space undergoes a random jump, and the timer is reset to zero. The second reset occurs based on an arbitrary timer-depended rate, and whenever this reset fires, the state-space is changed based on a given random map. We provide exact conditions for this class of systems that lead to finite statistical moments and the corresponding exact analytical expressions for the first two moments. This framework is applied to study random fluctuations in the concentration of a protein in a growing cell. In the context of this example, the timer denotes the time elapsed since the cell was born, and the cell division event (first reset) is triggered based on a timer-dependent rate. The second reset corresponds to the protein synthesis in stochastic bursts, and finally, during cell growth, protein concentration continuously decreases due to dilution. Our analysis provides closed-form formulas for the noise in the protein concentration and leads to a striking result - for a constant (timer-independent) protein synthesis rate, the noise in the protein concentration is invariant of the noise in the cell-cycle time. Finally, we provide a rigorous framework for investigating protein noise levels for different forms of timer-dependent synthesis rates, as is the case for cell-cycle regulated genes inside the cell.

Keywords: Stochastic hybrid systems, Systems biology, Hybrid and switched systems modeling, Cellular systems.

1. INTRODUCTION

This contribution focuses on Time-Triggered Stochastic Hybrid Systems, where the state evolves as per a linear dynamical system. This continuous-time evolution is interspersed by stochastic events that occur based on an internal timer. The timer measures the time elapsed since the last event and creates a memory in event timing. Whenever the event occurs, the state undergoes a random jump based on a given random map, and the timer is reset to zero. These SHS classes have been shown to be quite helpful in modeling and analyzing networked control systems (Antunes et al., 2013b,a; Hespanha, 2014; Soltani and Singh, 2018).

This work's key contribution is to generalize Time-Triggered SHS to include a second family of random resets (Fig. 1). This second family of resets occurs based on a timer-dependent rate, and similar to the first family of reset, the state undergoes a stochastic jump whenever the corresponding events occur. While the first family of resets reinitializes the timer back to zero, the second family of resets does not affect the timer. Note that these stochastic systems are essentially a subclass of Piecewise-deterministic Markov processes.

This work's second contribution is to use this framework for capturing random fluctuations in the concentration of a protein inside a cell that undergoes periods of growth followed by division into two daughters. Through our analysis, for the first time we predict the exact analytical formulas for the protein mean and noise levels when the protein synthesis rate varies arbitrarily along the cell cycle (E.g. as a function of the timer), giving novel results and insights that can be tested with further experiments.

This paper is organized as follows. In Section 2, we provide the mathematical formulation of the stochastic system and show its applicability in modeling protein concentration fluctuations inside an individual cell. In Section 3, we derive analytical formulas for the first and second-order moments for the general SHS system with two timer-dependent resets. These results are applied to the protein synthesis example in Section 4, followed by conclusions in

⋆ AS is supported by NSF (ECCS-1711548) and ARO (W911NF-19-1-0243).

10.1016/j.ifacol.2021.06.111

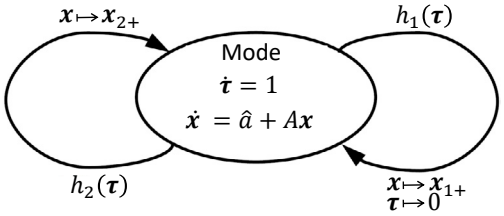

Fig. 1. **Model schematic of a stochastic hybrid system with two timer-dependent resets.** The state $\boldsymbol{x} \in \mathbb{R}^{n\times 1}$ evolves as per a linear time-invariant system and two families of resets occur at random times with rates $h_i(\boldsymbol{\tau}), i \in \{1, 2\}$. Here $\boldsymbol{\tau}$ is a timer that measures the time elapsed since the last event belonging to the first family of resets. Whenever the events occur the state is reset as per $\boldsymbol{x} \mapsto \boldsymbol{x}_{i^+}$, where $\boldsymbol{x}_{i^+}$ is a random variable whose statistics is given by (8) and (9). The first family of resets also reinitializes the timer back to zero, while the second family of resets has no impact on the timer.

Section 5. Before starting with the model formulation, we briefly discuss notation used throughout the paper.

Notation: $\mathbb{R}$ denotes the set of real numbers. We use hat to indicate constant vectors, e.g. $\hat{a}$, and matrices are denoted by capital letters. $A^\top$ is transpose of matrix A and I_n is $n \times n$ identity matrix. We use small bold letters to denote random processes. $\langle \boldsymbol{x} \rangle$ is expected value of random process $\boldsymbol{x}$. $\overline{\langle \boldsymbol{x} \rangle} \equiv \lim_{t\to\infty} \langle \boldsymbol{x} \rangle$ is the expected value at the steady-state. $\langle \boldsymbol{x} | \boldsymbol{y} \rangle$ is the conditional expectation of $\boldsymbol{x}$ given another random variable $\boldsymbol{y}$.

2. TIME-TRIGGERED STOCHASTIC HYBRID SYSTEMS

2.1 Model Formulation

The stochastic dynamical system is formulated as follows:

Continuous dynamics The states of the SHS $\boldsymbol{x} \in \mathbb{R}^{n\times 1}$ evolve as per a linear time-invariant system

$$\dot{\boldsymbol{x}}(t) = A\boldsymbol{x} + \hat{a}, \tag{1}$$

where $A \in \mathbb{R}^{n\times n}$ and $\hat{a} \in \mathbb{R}^{n\times 1}$ are constant matrix and vector, respectively. The continuous time evolution of the state space is interspersed by two families of random resets.

The first family of resets The first family of resets is assumed to occur at times $\boldsymbol{t}_s$, $s \in \{1, 2, 3, \ldots\}$, such that the time intervals $\boldsymbol{\tau_s} \equiv \boldsymbol{t}_s - \boldsymbol{t}_{s-1}$ are independent and identically distributed random variables following an arbitrary positively-valued continuous probability density function (pdf) f. To model the timing of these resets, we introduce a timer $\boldsymbol{\tau}$ that linearly increases over time

$$\dot{\boldsymbol{\tau}} = 1, \tag{2}$$

and resets to zero

$$\boldsymbol{\tau} \mapsto 0 \tag{3}$$

whenever a random event occurs. The occurrence of the next event depends on the state of the timer introducing memory in the event-arrival process. More specifically, the probability that an event occurs in the next infinitesimal time interval $(t, t+dt]$ is given by $h_1(\boldsymbol{\tau})dt$, where the *hazard rate* is

$$h_1(\tau) \equiv \frac{f(\tau)}{1 - \int_{y=0}^{\tau} f(y)dy}. \tag{4}$$

As an example, if f is exponentially-distributed with mean $\langle \boldsymbol{\tau_s} \rangle$, then $h_1(\tau) = 1/\langle \boldsymbol{\tau_s} \rangle$ would be a constant corresponding to Poisson arrival of events. Defining the arrival of events as per (4) ensures that $\boldsymbol{\tau_s}$ follows the pdf f

$$\boldsymbol{\tau_s} \sim f(\tau) = h_1(\tau) \mathrm{e}^{-\int_{y=0}^{\tau} h_1(y)dy}, \tag{5}$$

and the corresponding pdf of $\boldsymbol{\tau}$ is given by

$$\boldsymbol{\tau} \sim p(\tau) = \frac{1}{\langle \boldsymbol{\tau_s} \rangle} \mathrm{e}^{-\int_{y=0}^{\tau} h_1(y)dy}. \tag{6}$$

Having modeled the first family of resets' timing, we next describe its impact on the SHS state space. Each time this event occurs, the state of the system undergoes a random jump as per the reset

$$\boldsymbol{x} \mapsto \boldsymbol{x}_{1^+}, \boldsymbol{\tau} \mapsto 0, \tag{7}$$

where $\boldsymbol{x}_1^+$ represents the state of the system immediately after the event belonging to the first family of resets. We assume $\boldsymbol{x}_{1^+}$ to be a random variable whose statistics depend on the value of $\boldsymbol{x}$ just before the event. More specifically, the average value of $\boldsymbol{x}_1^+$ is

$$\langle \boldsymbol{x}_{1^+} \rangle = J_1\boldsymbol{x} + \hat{r}_1, \tag{8}$$

where $J_1 \in \mathbb{R}^{n\times n}$ and $\hat{r}_1 \in \mathbb{R}^{n\times 1}$ are constant matrix and vector, respectively. Furthermore, the covariance matrix $\boldsymbol{x}_1^+$ is given as

$$\langle \boldsymbol{x}_{1^+}\boldsymbol{x}_{1^+}^\top \rangle - \langle \boldsymbol{x}_{1^+} \rangle \langle \boldsymbol{x}_{1^+}^\top \rangle = Q_1 \boldsymbol{x}\boldsymbol{x}^\top Q_1^\top + B_1 \boldsymbol{x}\hat{c}_1^\top + \hat{c}_1 \boldsymbol{x} B_1^\top + G_1, \tag{9}$$

where $Q_1 \in \mathbb{R}^{n\times n}$, $B_1 \in \mathbb{R}^{n\times n}$ are constant matrices, $G_1 \in \mathbb{R}^{n\times n}$ is a constant symmetric positive semi-definite matrix, and $\hat{c}_1 \in \mathbb{R}^{n\times 1}$ is a constant vector. In essence, (9) represents the noise added when the event is triggered, and this noise can be state-dependent.

The second family of resets These resets occur randomly at a timer-dependent rate $h_2(\boldsymbol{\tau})$, where h_2 is an arbitrary positive-valued function, i.e., the probability that the second family of reset happens in the next infinitesimal time $(t, t + dt]$ is $h_2(\boldsymbol{\tau})dt$. Whenever these resets occur the state is reset as

$$\boldsymbol{x} \mapsto \boldsymbol{x}_{2^+}, \tag{10}$$

where $\boldsymbol{x}_{2^+}$ denotes the state of the system just after the event belonging to the second family of resets. Similar to (7), the average jump in $\boldsymbol{x}_{2^+}$ is

$$\langle \boldsymbol{x}_{2^+} \rangle = J_2\boldsymbol{x} + \hat{r}_2, \tag{11}$$

where $J_2 \in \mathbb{R}^{n\times n}$ and $\hat{r}_2 \in \mathbb{R}^{n\times 1}$ are constant matrix and vector, respectively. Furthermore, the covariance matrix of $\boldsymbol{x}_{2^+}$ is same as (9) by replacing Q_2, B_2, $\hat{c}_2$ and G_2 with Q_1, B_1, $\hat{c}_1$ and G_1 respectively. It is important to point out that unlike the first family of resets, the second family of resets *do not* affect the timer. While the occurrences of all stochastic events are timer driven, only events of the first family of resets reinitialize the timer back to zero (Fig. 1).

2.2 Biology Example

It turns out that the above SHS framework with two-timer dependent resets is ideal for capturing stochastic fluctuations in the concentration of a protein within growing cells.

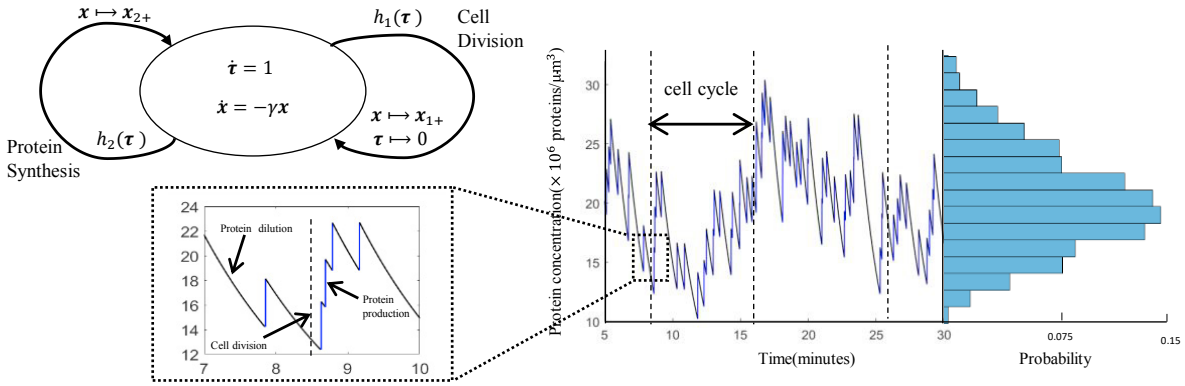

Fig. 2. **Modeling protein concentration in a single cell using the time-triggered stochastic hybrid system:** *Left*: Protein level $\boldsymbol{x}$ is modeled via an SHS with two families of stochastic resets. The first family of resets represents cell-division events that occur randomly with the rate $h_1(\boldsymbol{\tau})$ where $\boldsymbol{\tau}$ is cell-cycle timer measuring time elapsed since the cell was born. Whenever the cell divides, the protein level changes as per (14) and (15). The second family of resets corresponds to the production of proteins in bursts of size $\boldsymbol{u}$, and these burst events occur with the rate $h_2(\boldsymbol{\tau})$. For each burst event, the protein level changes as per (16) and (17). *Right*: Sample realization of the protein concentration showing increase due to burst events, exponential decay between two burst events due to dilution, and cell division events that do not change the mean concentration but add partitioning noise.

Before proceeding with a rigorous analysis of the SHS, we provide some details on this example.

Consider a newborn cell, whose volume grows exponentially over time with rate γ, and after a period of growth, the cell symmetrically divides into two daughters. These randomly-timed cell division events are the first family of resets. Here the timer $\boldsymbol{\tau}$ denotes the time elapsed since the cell's birth, and the next cell division event is assuming to occur with the rate $h_1(\boldsymbol{\tau})$. Choosing this rate as in (4) ensures that the time duration from cell birth to division $\boldsymbol{\tau_s}$ follows a prior probability distribution f. Let scalar $\boldsymbol{x}(t)$ denote the concentration of a protein. Then during cell growth, the protein level is continuously diluted as

$$\dot{\boldsymbol{x}}(t) = -\gamma \boldsymbol{x}, \tag{12}$$

where the growth rate is related to the average cell-cycle duration

$$\langle \boldsymbol{\tau_s} \rangle = \frac{\ln 2}{\gamma}. \tag{13}$$

This implies $A = -\gamma$, $\hat{a} = 0$ in (1). Note that a cell division event does not change the protein concentration (both the cell volume and the protein copy number are approximately halved). However, it introduces some noise due to errors from random partitioning of protein molecules between two daughters (Soltani et al., 2016; Huh and Paulsson, 2011b,a; Vahdat and Singh, 2021). Towards that end, the reset map for the first family of rests is given by

$$\langle \boldsymbol{x}_{1^+} \rangle = \boldsymbol{x} \tag{14}$$

and

$$\langle \boldsymbol{x}_{1^+}^2 \rangle - \langle \boldsymbol{x}_{1^+} \rangle^2 = b\boldsymbol{x}, \tag{15}$$

where the parameter b quantifies the extent of partitioning noise (Soltani et al., 2016). Comparing (14) and (15) with (8) and (9) leads to the following parameters for the first family resets: $J_1 = 1$, $B_1 = b/2$, $\hat{c}_1 = 1$ and $\hat{r}_1 = Q_1 = G_1 = 0$.

The second family of resets correspond to the stochastic synthesis of a protein in bursts as has been shown experimentally (Suter et al., 2011; Bartman et al., 2016; Singh et al., 2010), and modeled previously (Pedraza and Paulsson, 2008; Jia and Kulkarni, 2011; Kumar et al., 2015; Bokes and Singh, 2017; Vahdat et al., 2020; Shahrezaei and Swain, 2008; Friedman et al., 2006). In particular, the burst events arrive at rate $h_2(\boldsymbol{\tau})$ that can depend on the cell-cycle timer. Whenever the burst event occurs, the protein concentration increases by a burst size $\boldsymbol{u}$, where $\boldsymbol{u}$ is assumed to be an identically and independently distributed random variable. Based on this formulation of the second family of resets,

$$\langle \boldsymbol{x}_{2^+} \rangle = \boldsymbol{x} + \langle \boldsymbol{u} \rangle \tag{16}$$

and

$$\langle \boldsymbol{x}_{2^+}^2 \rangle - \langle \boldsymbol{x}_{2^+} \rangle^2 = \langle \boldsymbol{u}^2 \rangle - \langle \boldsymbol{u} \rangle^2, \tag{17}$$

implying $J_2 = 1$, $\hat{r}_2 = \langle \boldsymbol{u} \rangle$, $Q_2 = B_2 = \hat{c}_2 = 0$ and $G_2 = \langle \boldsymbol{u}^2 \rangle - \langle \boldsymbol{u} \rangle^2$. In summary, the SHS framework allows integration of three distinct noise mechanisms critically affecting gene expression: synthesis of a protein in random bursts, the division of a cell into two daughters at random times, and randomness in the partitioning of a protein between daughters. A typical stochastic realization of this SHS model is illustrated in Fig. 2.

3. STATISTICAL MOMENTS

Having formulated the SHS with two-timer dependent resets, we next derive the statistical moments of $\boldsymbol{x}$.

3.1 The first-order moment

We start by outlining our approach and then summarize the main result in Theorem 1. In between two successive events of the first family of resets, the conditional mean $\langle \boldsymbol{x} | \boldsymbol{\tau} = \tau \rangle$ evolves as follows (due to limited space, we provide the details in the OSF preprints version (Singh et al., 2019))

$$\frac{\partial \langle \boldsymbol{x} | \boldsymbol{\tau} = \tau \rangle}{\partial \tau} = A_x(\tau) \langle \boldsymbol{x} | \boldsymbol{\tau} = \tau \rangle + \hat{a}_x(\tau), \tag{18}$$

where

$$A_x(\tau) = A + h_2(\tau)(J_2 - I_n), \quad \hat{a}_x(\tau) = \hat{a} + h_2(\tau)\hat{r}_2. \tag{19}$$

This time-varying system leads to the following conditional mean

$$\begin{aligned}\langle \boldsymbol{x}|\boldsymbol{\tau} = \tau\rangle &= \mathrm{e}^{\int_0^\tau A_x(y)dy}\langle \boldsymbol{x}|\boldsymbol{\tau}=0\rangle \\ &+ \mathrm{e}^{\int_0^\tau A_x(y)dy}\int_0^\tau \mathrm{e}^{-\int_0^l A_x(y)dy}\hat{a}_x(l)dl,\end{aligned} \tag{20}$$

where $\langle \boldsymbol{x}|\boldsymbol{\tau}=0\rangle$ is the expected value just after the first family of resets. In order to find $\overline{\langle \boldsymbol{x}|\boldsymbol{\tau}=0\rangle}$, we apply (8)

$$\overline{\langle \boldsymbol{x}|\boldsymbol{\tau}=0\rangle} = J_1\overline{\langle \boldsymbol{x}|\boldsymbol{\tau}=\boldsymbol{\tau_s}\rangle} + \hat{r}_1, \tag{21}$$

and substitute $\langle \boldsymbol{x}|\boldsymbol{\tau}=\boldsymbol{\tau_s}\rangle$ from (20) in (21) that yields $\overline{\langle \boldsymbol{x}|\boldsymbol{\tau}=0\rangle}$. Finally, we use (6) to uncondition $\langle \boldsymbol{x}|\boldsymbol{\tau}=\tau\rangle$ with respect to $\boldsymbol{\tau}$ to get the expected value of $\boldsymbol{x}$. This result can be formally summarized as follows.

Theorem 1. Consider the SHS with two-timer dependent resets as formulated in (1)-(11). If all eigenvalues of $J_1\left\langle \mathrm{e}^{\int_0^{\boldsymbol{\tau_s}} A_x(y)dy}\right\rangle$ are inside the unit circle, then the first-order moment exists and is given by

$$\begin{aligned}\overline{\langle \boldsymbol{x}\rangle} &= \left\langle \mathrm{e}^{\int_0^{\boldsymbol{\tau}} A_x(y)dy}\right\rangle (I_n - J_1\left\langle \mathrm{e}^{\int_0^{\boldsymbol{\tau_s}} A_x(y)dy}\right\rangle)^{-1}\times \\ &\Big(J_1\left\langle \mathrm{e}^{\int_0^{\boldsymbol{\tau_s}} A_x(y)dy}\int_0^{\boldsymbol{\tau_s}} \mathrm{e}^{-\int_0^l A_x(y)dy}\hat{a}_x(l)dl\right\rangle + \hat{r}_1\Big) \\ &+ \left\langle \mathrm{e}^{\int_0^{\boldsymbol{\tau}} A_x(y)dy}\int_0^{\boldsymbol{\tau}} \mathrm{e}^{-\int_0^l A_x(y)dy}\hat{a}_x(l)dl\right\rangle,\end{aligned} \tag{22}$$

where

$$A_x(y) = A + h_2(y)(J_2 - I_n), \quad \hat{a}_x(y) = \hat{a} + h_2(y)\hat{r}_2. \tag{23}$$

■

A particular case of the Theorem is when $h_2(\boldsymbol{\tau}) = 0$ and the system reduces to a single family of resets as considered in (Soltani and Singh, 2019). For completeness, we provide this result as a Corollary.

Corollary 1. Assume that the system is described by (1)-(11) with $h_2(\boldsymbol{\tau}) = 0$ and all eigenvalues of the matrix $J_1\left\langle \mathrm{e}^{A\boldsymbol{\tau_s}}\right\rangle$ are inside the unit circle. Then the first order moment of the system is

$$\begin{aligned}\overline{\langle \boldsymbol{x}\rangle} &= \left\langle \mathrm{e}^{A\boldsymbol{\tau}}\right\rangle \left(I_n - J_1\langle \mathrm{e}^{A\boldsymbol{\tau_s}}\rangle\right)^{-1}\Big(J_1\left\langle \mathrm{e}^{A\boldsymbol{\tau_s}}\int_0^{\boldsymbol{\tau_s}} \mathrm{e}^{-Al}\hat{a}dl\right\rangle \\ &+ \hat{r}_1\Big) + \left\langle \mathrm{e}^{A\boldsymbol{\tau}}\int_0^{\boldsymbol{\tau}} \mathrm{e}^{-Al}\hat{a}dl\right\rangle.\end{aligned} \tag{24}$$

See the details for computing $\langle \mathrm{e}^{A\boldsymbol{\tau}}\rangle$ and $\left\langle \mathrm{e}^{A\boldsymbol{\tau_s}}\int_0^{\boldsymbol{\tau_s}} \mathrm{e}^{-Al}\hat{a}dl\right\rangle$ in (Vahdat et al., 2019).

3.2 Second-order moments

To derive the second-order moment we consider the time evolution of the conditioned covariance matrix $\left\langle \boldsymbol{x}\boldsymbol{x}^\top|\boldsymbol{\tau}\right\rangle$

$$\frac{\partial\left\langle \boldsymbol{x}\boldsymbol{x}^\top|\boldsymbol{\tau}\right\rangle}{\partial\tau} = A\boldsymbol{x}\boldsymbol{x}^\top + \boldsymbol{x}\boldsymbol{x}^\top A^\top + \hat{a}\boldsymbol{x}^\top + \boldsymbol{x}\hat{a}^\top. \tag{25}$$

By vectorization, we replace $\boldsymbol{x}\boldsymbol{x}^\top$ with $\mathrm{vec}(\boldsymbol{x}\boldsymbol{x}^\top)$. Defining

$$\boldsymbol{\mu} \equiv [\boldsymbol{x}^\top \ \mathrm{vec}(\boldsymbol{x}\boldsymbol{x}^\top)^\top]^\top, \tag{26}$$

the continuous dynamics of $\boldsymbol{\mu}$ follows

$$\dot{\boldsymbol{\mu}} = A_\mu\boldsymbol{\mu} + \hat{a}_\mu, \tag{27}$$

where

$$A_\mu = \left[\begin{array}{c:c} A & 0 \\ \hdashline I_n\otimes\hat{a} + \hat{a}\otimes I_n & I_n\otimes A + A\otimes I_n\end{array}\right], \ \hat{a}_\mu = \begin{bmatrix}\hat{a}\\ \hat{0}\end{bmatrix}, \tag{28}$$

and $\otimes$ denotes the Kronecker Product (Soltani and Singh, 2019). When the first family ($i = 1$) or the second family ($i = 2$) of resets occurs, $\boldsymbol{\mu}$ changes as per the map

$$\boldsymbol{\mu}_{i^+} = J_{\mu_i}\boldsymbol{\mu} + \hat{r}_{\mu_i}, i \in \{1, 2\}, \tag{29}$$

where

$$J_{\mu_i} = \left[\begin{array}{c:c} J_i & 0 \\ \hdashline \begin{array}{l}B_i\otimes\hat{c}_i + \hat{c}_i\otimes B_i \\ +J_i\otimes\hat{r}_i + \hat{r}_i\otimes J_i\end{array} & J_i\otimes J_i + Q_i\otimes Q_i\end{array}\right], \tag{30}$$

$$\hat{r}_{\mu_i} = \left[\begin{array}{c} \hat{r}_i \\ \hdashline \mathrm{vec}(G_i + \hat{r}_i\hat{r}_i^\top)\end{array}\right]. \tag{31}$$

Having recast the stochastic dynamics of $\boldsymbol{\mu}$, also as an SHS with two families of resets, the expected value of $\boldsymbol{\mu}$ (and hence $\boldsymbol{x}\boldsymbol{x}^\top$) can be obtained by applying Theorem 1 on this augmented system. While the analysis presented here is restricted to the first and second-order moments, a similar approach can be applied for deriving higher-order moments.

4. REVISITING STOCHASTIC PROTEIN SYNTHESIS

Having derived the first two moments of $\boldsymbol{x}$ in the general setting, we now revisit the biological example introduced in Section II. Recall that in the example, the scalar $\boldsymbol{x}$ denote the concentration of a protein that is continuously diluted from cell growth via (12). The first family of resets represents cell-division events that reset the state as per (14) and (15). The second family of resets corresponds to protein bursts that reset the state as per (16) and (17).

Defining the vector $\boldsymbol{\mu} \equiv [\boldsymbol{x} \ \ \boldsymbol{x}^2]^\top$, then the continuous dynamics of $\boldsymbol{\mu}$ between resets is given by (27) with

$$A_\mu = \begin{bmatrix}-\gamma & 0\\ 0 & -2\gamma\end{bmatrix}, \ \hat{a}_\mu = \begin{bmatrix}0\\0\end{bmatrix}. \tag{32}$$

Using (29), the resets in $\boldsymbol{\mu}$ are

$$J_{\mu_1} = \begin{bmatrix}1 & 0\\ b & 1\end{bmatrix}, \ \hat{r}_{\mu_1} = \begin{bmatrix}0\\0\end{bmatrix}, \tag{33}$$

$$J_{\mu_2} = \begin{bmatrix}1 & 0\\ 2\langle \boldsymbol{u}\rangle & 1\end{bmatrix}, \ \hat{r}_{\mu_2} = \begin{bmatrix}\langle \boldsymbol{u}\rangle\\ \langle \boldsymbol{u}^2\rangle\end{bmatrix} \tag{34}$$

corresponding to the first and second families of resets, respectively. Applying Theorem 1 on this augmented system yields the first two steady-state moments of the protein concentration. As the formula for the second-order moment is quite lengthy, we only provide the result for the mean protein concentration that is given by

$$\overline{\langle \boldsymbol{x}\rangle} = \frac{\langle \boldsymbol{u}\rangle}{\gamma\langle \boldsymbol{\tau_s}\rangle}\left\langle \mathrm{e}^{-\gamma\boldsymbol{\tau_s}}\int_0^{\boldsymbol{\tau_s}} \mathrm{e}^{\gamma l}h_2(l)dl\right\rangle + \langle \boldsymbol{u}\rangle\left\langle \mathrm{e}^{-\gamma\boldsymbol{\tau}}\int_0^{\boldsymbol{\tau}} \mathrm{e}^{\gamma l}h_2(l)dl\right\rangle \tag{37}$$

with $\langle \boldsymbol{u}\rangle$ being the mean burst size, γ the protein dilution rate, and $h_2(\boldsymbol{\tau})$ the timer-dependent protein synthesis rate. Next, we explore protein mean and noise levels for specific forms of the synthesis rate. We quantify protein noise levels by the steady-state Fano factor $FF_{\boldsymbol{x}}$ (variance/mean).

$$FF_{\boldsymbol{x}} = \underbrace{\frac{\langle \boldsymbol{u}^2\rangle}{2\langle \boldsymbol{u}\rangle}}_{\text{Protein bursting noise}} + \underbrace{b\left(\frac{k_2\langle \boldsymbol{\tau_s}\rangle(\langle e^{-\gamma\boldsymbol{\tau_s}}\rangle - 1 + \ln(2))}{(1-\langle e^{-\gamma\boldsymbol{\tau_s}}\rangle)\ln^2(2)((CV^2_{\boldsymbol{\tau_s}}+1)k_2\langle \boldsymbol{\tau_s}\rangle + 2k_1)} + \frac{k_1}{\ln(2)((CV^2_{\boldsymbol{\tau_s}}+1)k_2\langle \boldsymbol{\tau_s}\rangle + 2k_1)}\right)}_{\text{Partitioning noise}} + \underbrace{\frac{\langle \boldsymbol{u}\rangle k_2{}^2\left((1-\langle e^{-\gamma\boldsymbol{\tau_s}}\rangle)\langle \boldsymbol{\tau_s}\rangle^3\left(3(CV^2_{\boldsymbol{\tau_s}}+1)^2\ln^2(2)+6(CV^2_{\boldsymbol{\tau_s}}+1)\ln(2)-12\right)+4(\langle e^{-\gamma\boldsymbol{\tau_s}}\rangle - 1)\langle \boldsymbol{\tau_s}^3\rangle\ln^2(2)+12\langle \boldsymbol{\tau_s} e^{-\gamma\boldsymbol{\tau_s}}\rangle\langle \boldsymbol{\tau_s}\rangle^2\ln(2)\right)}{6(\langle e^{-\gamma\boldsymbol{\tau_s}}\rangle - 1)\ln^3(2)((CV^2_{\boldsymbol{\tau_s}}+1)k_2\langle \boldsymbol{\tau_s}\rangle + 2k_1)}}_{\text{Cell-cycle noise}}. \tag{44}$$

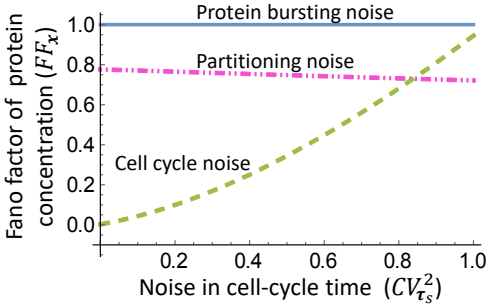

Fig. 3. **Protein noise components are affected differently by the noise in the cell-cycle time.** For a Gamma-distributed $\boldsymbol{\tau_s}$, the noise components in (44) are plotted with respect to $CV^2_{\boldsymbol{\tau_s}}$. Interestingly contrasting behaviors emerge with the noise contribution from bursting remaining constant, the noise contribution from partitioning decreasing, and the noise contribution from cell-cycle noise increasing as $CV^2_{\boldsymbol{\tau_s}}$ varies from zero (deterministic cell-cycle times) to one (exponentially distributed cell-cycle times). Other parameters taken as $\langle \boldsymbol{\tau_s}\rangle = 1\ hr$, $\langle \boldsymbol{u}^2\rangle = 2$, $\langle \boldsymbol{u}\rangle = 1$, $b = 1$, $k_1 = 1\ hr^{-1}$, $k_2 = 2\ hr^{-2}$.

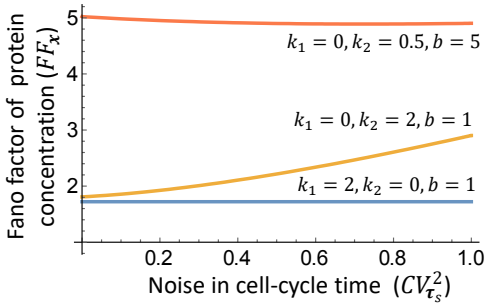

Fig. 4. **Depending on the protein synthesis rate and partitioning noise, noise in protein concentration may decrease, increase or remain invariant of the noise in the cell-cycle timing.** Steady-state Fano factor of protein concentration as a function of the noise in the cell-cycle timing for a Gamma-distributed $\boldsymbol{\tau_s}$ and synthesis rate (42). If the coefficient k_2 is zero, $FF_{\boldsymbol{x}}$ remains constant with respect to changes in $CV^2_{\boldsymbol{\tau_s}}$. For other values of k_2 and k_1, $FF_{\boldsymbol{x}}$ depends on the value of b. Other parameters are taken as $\langle \boldsymbol{\tau_s}\rangle = 1\ hr$, $\langle \boldsymbol{u}^2\rangle = 2$, $\langle \boldsymbol{u}\rangle = 1$.

4.1 Constant protein synthesis rate

For a constant protein synthesis rate

$$h_2(\boldsymbol{\tau}) = k_1, \tag{39}$$

using (13) into (37) we get

$$\overline{\langle \boldsymbol{x}\rangle} = \frac{k_1\langle \boldsymbol{u}\rangle\langle \boldsymbol{\tau_s}\rangle}{\ln(2)}. \tag{40}$$

Moreover, the steady-state Fano factor of the protein concentration obtained as

$$FF_{\boldsymbol{x}} = \underbrace{\frac{\langle \boldsymbol{u}^2\rangle}{2\langle \boldsymbol{u}\rangle}}_{\text{Protein bursting noise}} + \underbrace{\frac{b}{2\ln(2)}}_{\text{Partitioning noise}}. \tag{41}$$

The first component represents the contribution from stochastic bursting, and the second component arises due to partitioning errors at the time of cell division. It is remarkable that in this case the Fano factor is independent of k_1, γ and the moments of the cell-cycle time $\boldsymbol{\tau_s}$.

4.2 Linearly increasing protein synthesis rate

We next assume that the protein synthesis rate is a linear increasing function of $\boldsymbol{\tau}$

$$h_2(\boldsymbol{\tau}) = k_2\boldsymbol{\tau} + k_1, \tag{42}$$

with positive constants k_1 and k_2. Then, using a similar procedure we obtain

$$\overline{\langle \boldsymbol{x}\rangle} = \frac{k_1\langle \boldsymbol{u}\rangle\langle \boldsymbol{\tau_s}\rangle}{\ln(2)} + \frac{k_2\langle \boldsymbol{u}\rangle(CV^2_{\boldsymbol{\tau_s}}+1)\langle \boldsymbol{\tau_s}\rangle^2}{2\ln(2)}, \tag{43}$$

which depends on the average cell-cycle duration $\langle \boldsymbol{\tau_s}\rangle$, and interestingly, also depends on the noise in cell-cycle time $CV^2_{\boldsymbol{\tau_s}}$ as quantified by its coefficient of variation squared. The Fano factor of the protein concentration is given by (44) on the top of this page. It can be decomposed into three components representing contributions from stochastic bursting, partitioning noise, and cell cycle noise.

To get some insight into how these components vary with $CV^2_{\boldsymbol{\tau_s}}$, we consider a Gamma-distributed $\boldsymbol{\tau_s}$. For this purpose, the terms $\langle e^{-\gamma\boldsymbol{\tau_s}}\rangle$, $\langle \boldsymbol{\tau_s} e^{-\gamma\boldsymbol{\tau_s}}\rangle$ and $\langle \boldsymbol{\tau_s}^3\rangle$ in (44) are further simplified and provided in the OSF preprints version (Singh et al., 2019). In Fig. 3, we plot the three different noise components of Fano factor from (44) as a function of $CV^2_{\boldsymbol{\tau_s}}$ and observe contrasting behaviors – the noise contribution from bursting remains constant, the noise contribution from partitioning decreases, and finally, the noise contribution from cell-cycle noise increases. Fig. 4 plots the overall Fano factor as a function of $CV^2_{\boldsymbol{\tau_s}}$ and depending on the relative contributions, it can either remain constant, monotonically increase, or vary non-monotonically with $CV^2_{\boldsymbol{\tau_s}}$.

5. CONCLUSION

We formulated a class of time-triggered stochastic hybrid systems with two families of resets and exploited this framework to investigate the noise in the concentration of a given protein. Our analysis provides the first results connecting the protein mean and noise levels to distinct noise mechanisms (stochastic bursting, noise in the cell-

cycle time, and randomness in partitioning of molecules between two cells). A key highlight of our results is that the protein level's noise becomes invariant of both the mean cell cycle time and the noise in the cell cycle time for a constant protein production rate. This natural buffering of protein noise levels to the cell cycle is intriguing and can be experimentally tested by measuring protein noise levels for changing growth conditions in a given cell type.

When the protein production is timer-dependent, we derive exact analytical formulas for the statistical moments of $\boldsymbol{x}$. In this case, the protein level noise can be decomposed into three components corresponding to the three different noise mechanisms. Our analysis shows that the noise component from bursting is invariant of $\boldsymbol{\tau_s}$, the noise component for partitioning slightly decreases with increasing noise $CV^2_{\boldsymbol{\tau_s}}$, and finally the noise contribution from cell cycle increases sharply with $CV^2_{\boldsymbol{\tau_s}}$. While the analysis here was restricted to a simple linear production rate $h_2(\boldsymbol{\tau}) = k_2\boldsymbol{\tau}+k_1$, we plan to investigate more complex functions in the future.

In (Vahdat and Singh, 2021), we solved the closed-form statistical moments for a TTSHS with nonlinear continuous dynamics. So, an interesting future work would be expanding the two-timer TTSHS model to include nonlinear continuous dynamics. Another interesting direction of future work is to consider two families of resets, each having its own individual timers. For example, recent work has shown that the time interval between two protein burst events follows non-exponential statistical distributions (Daigle et al., 2015). Thus, by having a second timer, we can capture a memory in the timing of the burst events. In future work, we will expand this analysis to multi-mode SHS, allowing for timer-based switching between stochastic dynamical systems.

ACKNOWLEDGMENT

This work is supported by grants from the Army Research Office (W911NF1910243) and the National Science Foundation (ECCS-1711548).

REFERENCES

Antunes, D., Hespanha, J., and Silvestre, C. (2013a). Stability of networked control systems with asynchronous renewal links: An impulsive systems approach. *Automatica*, 49, 402–413.

Antunes, D., Hespanha, J.P., and Silvestre, C. (2013b). Stochastic hybrid systems with renewal transitions: Moment analysis with application to networked control systems with delays. *SIAM Journal on Control and Optimization*, 51, 1481–1499.

Bartman, C.R., Hsu, S.C., Hsiung, C.C.S., Raj, A., and Blobel, G.A. (2016). Enhancer regulation of transcriptional bursting parameters revealed by forced chromatin looping. *Molecular Cell*, 62, 237 – 247.

Bokes, P. and Singh, A. (2017). Gene expression noise is affected deferentially by feedback in burst frequency and burst size. *Journal of Mathematical Biology*, 74, 1483–1509.

Daigle, B., Soltani, M., Petzold, L., and Singh, A. (2015). Inferring single-cell gene expression mechanisms using stochastic simulation. *Bioinformatics*, 31, 1428–1435.

Friedman, N., Cai, L., and Xie, X. (2006). Linking stochastic dynamics to population distribution: an analytical framework of gene expression. *Physical Review Letters*, 97, 168302.

Hespanha, J.P. (2014). Modeling and analysis of networked control systems using stochastic hybrid systems. *Annual Reviews in Control*, 38, 155–170.

Huh, D. and Paulsson, J. (2011a). Non-genetic heterogeneity from stochastic partitioning at cell division. *Nature Genetics*, 43, 95–100.

Huh, D. and Paulsson, J. (2011b). Random partitioning of molecules at cell division. *Proceedings of the National Academy of Sciences*, 108(36), 15004–15009. doi: 10.1073/pnas.1013171108.

Jia, T. and Kulkarni, R.V. (2011). Intrinsic noise in stochastic models of gene expression with molecular memory and bursting. *Journal of Mathematical Biology*, 106, 058102.

Kumar, N., Singh, A., and Kulkarni, R.V. (2015). Transcriptional bursting in gene expression: analytical results for general stochastic models. *PLOS Computational Biology*, 11, e1004292.

Pedraza, J.M. and Paulsson, J. (2008). Effects of molecular memory and bursting on fluctuations in gene expression. *Science*, 319, 339 – 343.

Shahrezaei, V. and Swain, P.S. (2008). Analytical distributions for stochastic gene expression. *Proceedings of the National Academy of Sciences*, 105, 17256–17261.

Singh, A., Razooky, B., Cox, C.D., Simpson, M.L., and Weinberger, L.S. (2010). Transcriptional bursting from the HIV-1 promoter is a significant source of stochastic noise in HIV-1 gene expression. *Biophysical Journal*, 98, L32–L34.

Singh, A., Vahdat, Z., and Xu, Z. (2019). Time-triggered stochastic hybrid systems with two timer-dependent resets. *OSF Preprints*.

Soltani, M., Vargas-Garcia, C.A., Antunes, D., and Singh, A. (2016). Intercellular variability in protein levels from stochastic expression and noisy cell cycle processes. *PLOS Computational Biology*, e1004972.

Soltani, M. and Singh, A. (2018). Control design and analysis of a stochastic event-driven system. *IEEE Conference on Decision and Control (CDC)*, 5789–5794.

Soltani, M. and Singh, A. (2019). Moment analysis of linear time-varying dynamical systems with renewal transitions. *SIAM Journal on Control and Optimization*, 57(4), 2660–2685.

Suter, D.M., Molina, N., Gatfield, D., Schneider, K., Schibler, U., and Naef, F. (2011). Mammalian genes are transcribed with widely different bursting kinetics. *Science*, 332, 472–474.

Vahdat, Z., Nienałtowski, K., Farooq, Z., Komorowski, M., and Singh, A. (2020). Information processing in unregulated and autoregulated gene expression. In *2020 European Control Conference (ECC)*, 258–263. IEEE.

Vahdat, Z. and Singh, A. (2021). Time triggered stochastic hybrid system with nonlinear continuous dynamics. *OSF Preprints*.

Vahdat, Z., Xu, Z., and Singh, A. (2019). Modeling and characterization of neuronal synapses using stochastic hybrid systems. *IEEE 58th Annual Conference on Decision and Control (CDC)*.